Polymer 51 (2010) 4225–4230

Contents lists available at ScienceDirect

Polymer

journal homepage: www.elsevier.com/locate/polymer

Effect of solvent evaporation rate on the crystalline state of electrospun Nylon 6

Carl B. Giller, D. Bruce Chase, John F. Rabolt*, Christopher M. Snively**

University of Delaware, Department of Materials Science and Engineering, Newark, DE 19716, USA

ARTICLE INFO

Article history:
Received 28 May 2010
Accepted 30 June 2010
Available online 7 July 2010

Keywords:
Nylon 6
Electrospinning kinetics
Crystalline state

ABSTRACT

The role of solvent evaporation on the crystalline state of electrospun Nylon 6 fibers was examined by electrospinning into a closed chamber filled with different concentrations of solvent vapor. It was found that the thermodynamically stable α form became increasingly dominant in Nylon 6 fibers electrospun out of both 1,1,1,3,3,3-hexafluoro-2-propanol (HFIP) and formic acid as the vapor phase solvent concentration increased. It is believed that the formation of the metastable γ form is due in part to the fast solvent evaporation kinetics associated with the electrospinning process. By varying the vapor phase concentration and thus the rate of solvent evaporation during electrospinning, we were able to vary the resulting crystal structure of the electrospun Nylon 6, as shown by XRD, Raman and FTIR.

1. Introduction

Nylon 6 is known to exist in two well characterized crystal forms. The structure of the α form consists of adjacent polymer chains oriented in opposite directions relative to each other (anti-parallel) [1], thereby maximizing hydrogen bonding interactions. It is the more thermodynamically stable of the two crystal forms due to the optimized hydrogen bonding interactions in this structure. The γ form consists of adjacent Nylon 6 chains oriented parallel to each other, resulting in less efficient hydrogen bonding and thus a less thermodynamically favorable (metastable) crystalline form. It was additionally found [2,3] that the α form could be transformed to the γ form upon soaking the α form with an aqueous KI/I_2 solution, followed by rinsing with an aqueous $Na_2S_2O_3$ solution.

Electrospinning, an electrostatically driven polymer processing method that can produce polymer fibers with diameters ranging from nanometers to microns, has been extensively employed to produce non-woven fibrous mats of both synthetic and naturally occurring polymers [4,5]. Nylon 6 [6–8] and Nylon 6 composites [9,10] have been processed via this method. The key finding from these studies is that while the melt processed polymer [7,10] and films cast from the solutions used to electrospin [8] exhibited the α form, electrospinning resulted in the metastable γ form [6–8,10]. Electrospun fibers of other polymorphic polymers such as spider silk [11] and poly(1-butene) [12] show similar polymorphic behavior. The proposed mechanism for this molecular transformation has centered on the interaction of the applied electric field with polar groups in the polymer [11,13], but with no detailed supporting evidence. The electric fields typically employed in electrospinning [5] are only on the order of 1 kV/cm, which is too weak to induce molecular alignment [14]. We propose that the polymorphic behavior stems in part from a balance between the rates of crystallization and solvent evaporation. In this scheme, an evaporation rate faster than the crystallization rate of the thermodynamically stable α form would help induce the metastable γ form, whereas slower evaporation rates would result in the α form. Nylon 6 was electrospun in an environmental chamber filled with varying amounts of solvent vapor to control the evaporation rate. Field emission scanning electron microscopy (FE-SEM), wide angle X-ray scattering (WAXS), Raman spectroscopy, and Fourier transform infrared (FTIR) spectroscopy were employed to examine the electrospun materials in this study.

2. Experimental

HFIP (Sigma Aldrich) and formic acid (98+%, pure, Acros Organics) were used as received. Nylon 6 (Sigma Aldrich, MW = 10,000 Da) was heated to 110 °C (well above its T_g of 62.5 °C) for 2.5 h to remove excess residual moisture. 18% (w/w) Nylon 6 solutions in formic acid and 6% (w/w) Nylon 6 solutions in HFIP were prepared and stirred for at least 18 h prior to use. These concentrations were optimized for the reproducible production of smooth, uniform fiber morphologies [15]. A 25.40 × 27.31 × 30.48 cm glass box (GlassCages.com, LLC) was used as the environmental chamber. Prior to electrospinning, a specific amount of solvent was dispensed into a glass beaker inside the environmental chamber.

* Corresponding author. Tel.: +1 (302)831 4476; fax: +1 (302)831 4545.
** Corresponding author. Present address: SCHOTT North America, Inc. Tel.: +1 (570)457 7485x420.
E-mail addresses: rabolt@udel.edu (J.F. Rabolt), christopher.snively@us.schott.com (C.M. Snively).

0032-3861/$ – see front matter © 2010 Elsevier Ltd. All rights reserved.
doi:10.1016/j.polymer.2010.06.057

A heating cartridge placed in the beaker and a fan placed above the beaker were used to evaporate the solvent and distribute it throughout the chamber. After all of the solvent was visibly evaporated, 5 min were allowed to elapse before electrospinning was initiated.

For all electrospinning experiments, a +12 kV potential was applied to the needle and a −4 kV potential was applied to the collector. Solutions were electrospun from a syringe attached to a 21 gauge needle (Small Parts, Inc.) with a working distance of 10 cm. The temperature and relative humidity (RH) ranged from 20 °C to 22 °C and 14%–55%, respectively, during the course of the experiments. For comparison purposes, films were cast from the solutions used to electrospin, and some of these were subsequently treated with an aqueous KI/I_2 solution, followed by rinsing with an aqueous $Na_2S_2O_3$ solution [2,16] to induce formation of the γ form.

Images of the electrospun Nylon 6 were acquired with a JEOL JSM-7400 Field Emission Scanning Electron Microscope using a 2 kV electron beam operating at 10 μA. FTIR spectra were obtained using a Thermo Nicolet Nexus 670 FTIR spectrometer operating in transmission mode (4000 cm^{-1} to 650 cm^{-1} spectral range, 4 cm^{-1} resolution, 128 scans). Raman spectra were acquired using a Kaiser Optical Systems, Inc. (Ann Arbor, Michigan) Holospec VPT System and an Invictus diode laser with 785 nm excitation. For all Raman spectra, background spectra from the probehead were subtracted out and the resultant spectra were corrected for instrument response. Wide angle X-ray scattering profiles were acquired on a Rigaku D-Max B diffractometer using CuK_α X-rays ($\lambda = 1.54$ Å) over the range of $5^\circ \leq 2\theta \leq 50^\circ$ with a 0.05° step size and a 4 s dwell time.

3. Results

Nylon 6/HFIP solutions were electrospun inside the environmental chamber with HFIP vapor phase concentrations ranging from 0 to 284 g/m^3. In addition, a control sample of the same solution was electrospun outside of the environmental chamber under ambient conditions. FE-SEM images of these materials are shown in Fig. 1. For Nylon 6 electrospun outside of the environmental chamber, the fibers appear well-defined with diameters of roughly a few hundred nanometers. The same morphology is observed for the materials electrospun inside the chamber with no added solvent and with an HFIP concentration of 35 g/m^3 (not shown). As the concentration of HFIP is increased to 71 g/m^3, a slightly fused morphology is noticeable (not shown), and becomes even more apparent at a concentration of 106 g/m^3. Increasing the concentration of evaporated HFIP to 142 or 213 g/m^3 in the chamber results in a highly fused morphology, with few distinct fibers being observed. This trend in morphology can be understood by considering that it becomes increasingly difficult for the electrospun material to completely dry before it hits the collector as the atmosphere becomes more concentrated with solvent. Attempts to electrospin this solution at an HFIP concentration of 284 g/m^3 resulted in a morphology similar to that achieved via electrospraying, further validating this hypothesis.

An analysis of these materials on the molecular level shows even more dramatic changes as the amount of evaporated solvent inside the environmental chamber is increased. Fig. 2 shows the X-ray profiles of Nylon 6 electrospun with different concentrations of HFIP in the chamber. In addition, the profiles acquired from a solvent cast film with and without KI/I_2 treatment are shown for comparison. It is well established that solvent cast films of Nylon 6 consist primarily of the α form [8], and the KI/I_2 treated film consists mainly of the γ form [2,3,7]. Observing the profiles in Fig. 2, it is apparent that, as the amount of evaporated solvent inside the chamber increases, the crystal structure of Nylon 6 gradually transforms from γ to α, as seen in the strong $(200)_\gamma$ reflection at $2\theta = 21.5^\circ$ splitting into the $(200)_\alpha$ and $(002)_\alpha/(202)_\alpha$ reflections at $2\theta = 20.4^\circ$ and 24.1°, respectively [6,8]. The lack of the $(020)_\gamma$ reflection at $2\theta = 10.8^\circ$ in the profiles in which the $(200)_\gamma$ splitting occurs further validates this observation. However, the lack of this reflection even in the profiles of electrospun material possessing the unsplit $(200)_\gamma$ reflection has been observed in earlier studies [17–19] of Nylon 6 films, but with no clear explanation.

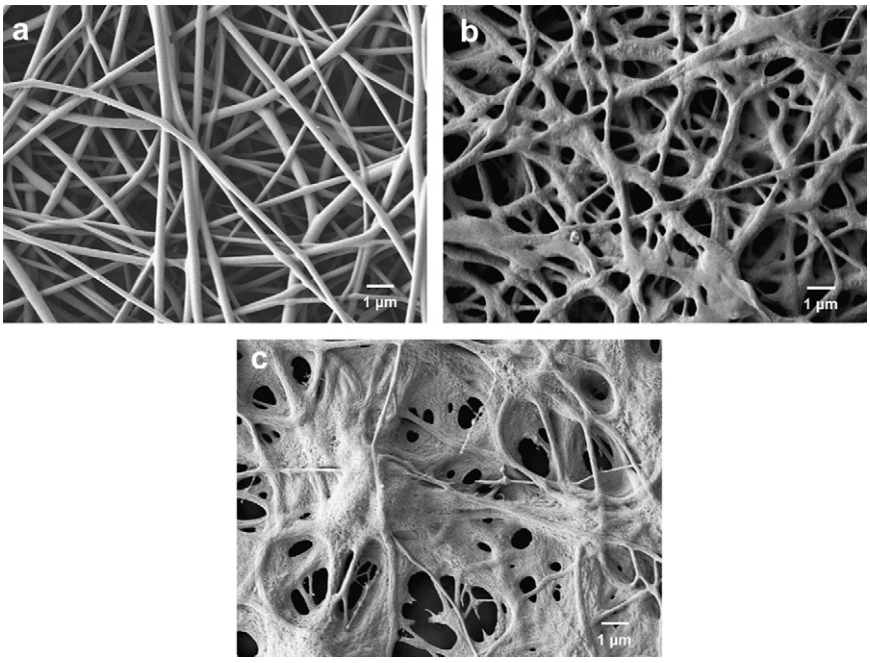

Fig. 1. FE-SEM images of Nylon 6 electrospun (a) without the environmental chamber, and at HFIP vapor phase concentrations in the chamber of (b) 106 g/m^3 and (c) 213 g/m^3. The scale bar for all three images is 1 μm.

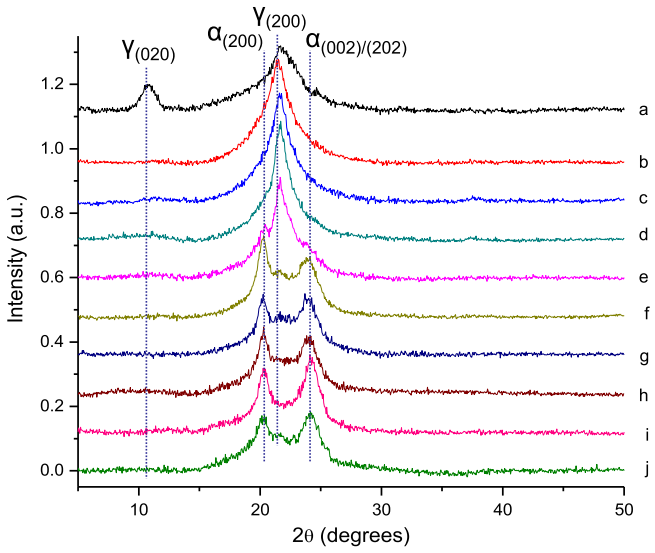

Fig. 2. X-ray profiles of Nylon 6 processed from HFIP: (a) KI/I_2 treated cast film; fibers electrospun (b) without the environmental chamber and with varying concentrations of evaporated HFIP: (c) 0 g/m^3, (d) 35 g/m^3, (e) 71 g/m^3, (f) 106 g/m^3, (g) 123 g/m^3, (h) 142 g/m^3, (i) 213 g/m^3; and (j) a solvent cast film.

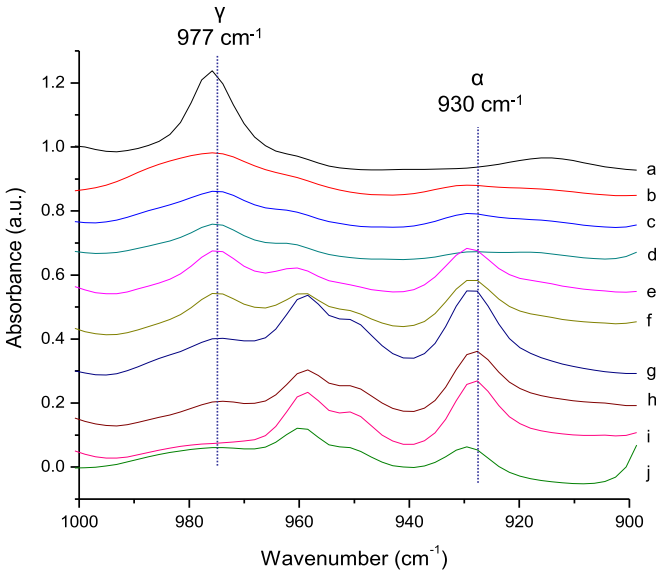

Fig. 4. FTIR spectra of Nylon 6 processed from HFIP: (a) KI/I_2 treated cast film; fibers electrospun (b) without the environmental chamber and with varying concentrations of evaporated HFIP: (c) 0 g/m^3, (d) 35 g/m^3, (e) 71 g/m^3, (f) 106 g/m^3, (g) 123 g/m^3, (h) 142 g/m^3, (i) 213 g/m^3; and (j) a solvent cast film.

Vibrational spectroscopy, which is sensitive to the molecular conformation of polymers [20,21], also shows similar trends to those of the X-ray profiles. Fig. 3 shows the Raman spectra of Nylon 6 electrospun fibers with different concentrations of HFIP in the chamber, in addition to the α and γ form cast films. As the amount of evaporated solvent increases, the C–C stretching bands at 1060 cm^{-1} and 1127 cm^{-1}, indicative of the trans planar CC conformation found in the α form, gradually increase in intensity relative to the 1076 cm^{-1} band, indicative of the gauche CC conformation typically found in the γ form [7]. In addition, the two C–N–H bending vibrations at 1467 cm^{-1} and 1477 cm^{-1}, also indicative of the trans amide conformation in the α form, steadily increase in intensity [7]. The FTIR spectra in Fig. 4 reveal a similar

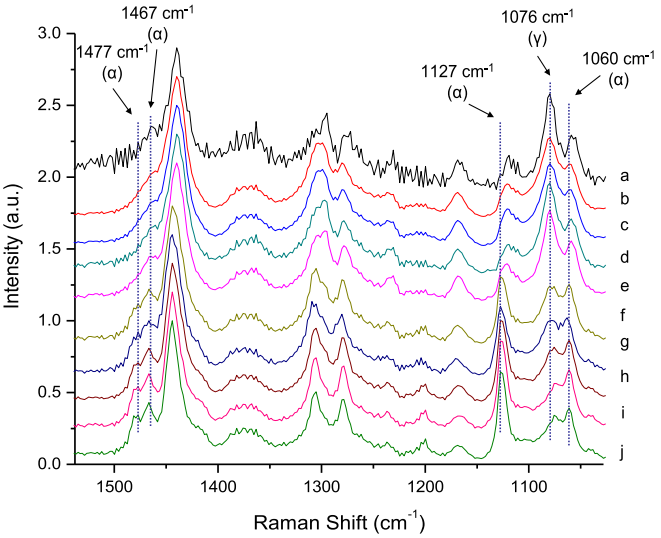

Fig. 3. Raman spectra of Nylon 6 processed from HFIP: (a) KI/I_2 treated cast film; fibers electrospun (b) without the environmental chamber and with varying concentrations of evaporated HFIP: (c) 0 g/m^3, (d) 35 g/m^3, (e) 71 g/m^3, (f) 106 g/m^3, (g) 123 g/m^3, (h) 142 g/m^3, (i) 213 g/m^3; and (j) a solvent cast film. All spectra were normalized relative to the 1440 cm^{-1} CH_2 bending vibration.

pattern. All of the spectra were normalized relative to the CO–NH skeletal motion mode at 1170 cm^{-1}, which has previously been demonstrated [22] to be independent of the density, and thus the crystallinity, of Nylon 6. The smooth increase in the CO–NH bending mode at 930 cm^{-1} (characteristic of the α form) relative to the CO–NH bending mode at 977 cm^{-1} (characteristic of the γ form) with increasing amounts of evaporated solvent further confirms this behavior [22,23].

Nylon 6 fibers electrospun from formic acid solutions were also studied to provide further evidence that solvent evaporation kinetics plays a significant role in the observed molecular transformation, irrespective of the solvent used. FE-SEM images of electrospun Nylon 6 fibers processed in the environmental chamber containing different concentrations of formic acid are shown in Fig. 5. Unlike the case of HFIP, the surface morphology of the fibers did not change appreciably over the range of evaporated formic acid, and well-defined fibers were formed for all solvent vapor concentrations.

The X-ray, Raman, and FTIR results for Nylon 6 electrospun with varying amounts of evaporated formic acid are shown in Figs. 6,7 and 8, respectively. These results display the same trend as that seen for HFIP. However, upon closer examination of the X-ray data in Fig. 6 for the material electrospun at a formic acid concentration of 189 g/m^3, one can clearly see that the γ form, which has a strong reflection at $2\theta = 21.5°$ [6,8], does not completely disappear. Increasing the evaporated formic acid concentration resulted in the disappearance of the γ peak.

4. Discussion

It is well documented that, while electrospinning Nylon 6 results in the formation of the metastable γ form [6–8,10], solvent casting films from the same solution results in the formation of the more thermodynamically stable α form [8]. This is not surprising, since the two processes have dramatically different solvent evaporation kinetics. The whipping instability in electrospinning, which results in the elongation of the polymer solution jet and subsequent solvent evaporation, has been shown to occur on the order of milliseconds [24,25], whereas evaporation in solvent cast films can

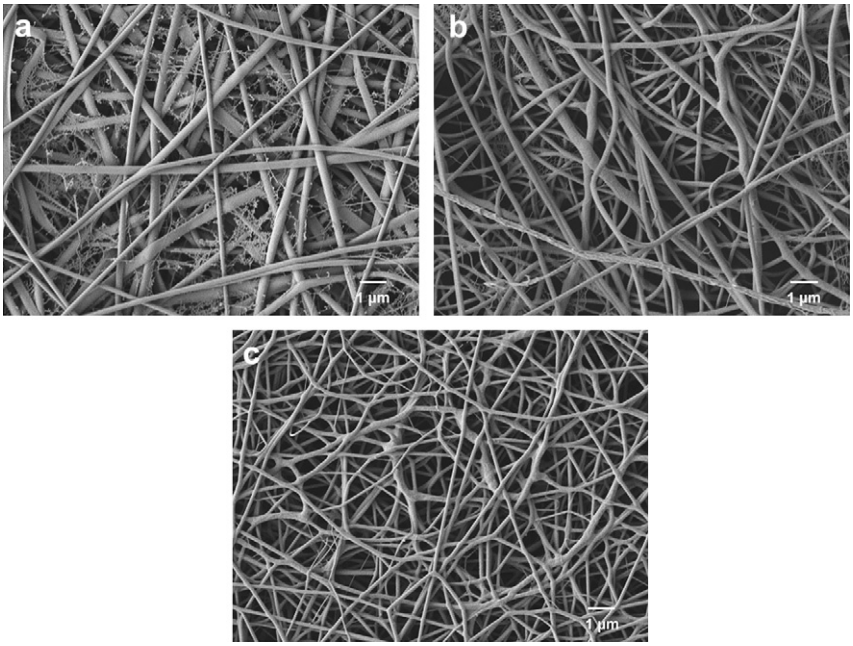

Fig. 5. FE-SEM images of Nylon 6 electrospun (a) without the environmental chamber, and at formic acid vapor phase concentrations in the chamber at (b) 114 g/m^3 and (c) 227 g/m^3. The scale bar for all three images is 1 μm.

take anywhere from minutes to hours, depending on film thickness and mass transport.

From these experiments, the amount of α form was correlated to the solvent vapor concentration in the chamber. Because all materials were electrospun at the same electric field strength, the fact that the γ to α transition was more complete as more solvent was evaporated into the electrospinning atmosphere strongly indicates that solvent evaporation kinetics significantly impact the crystal structure of the resultant polymer. At greater solvent vapor concentrations, it is very likely that the polymer chains have more time to pack into the thermodynamically stable α form, suggesting that the solvent evaporation kinetics inherent to the electrospinning process drastically slows down under these conditions. This is further supported by the observed fused morphology of the materials. At lower concentrations of evaporated solvent, our data suggests the solvent evaporation rate is faster than the crystallization rate of the α form, and the resultant electrospun Nylon 6 is kinetically trapped in the metastable γ form.

Although these results suggest that the crystalline state of electrospun Nylon 6 is largely dependent on the solvent evaporation kinetics during electrospinning, which depends on the solvent vapor concentration in the environmental chamber, it is

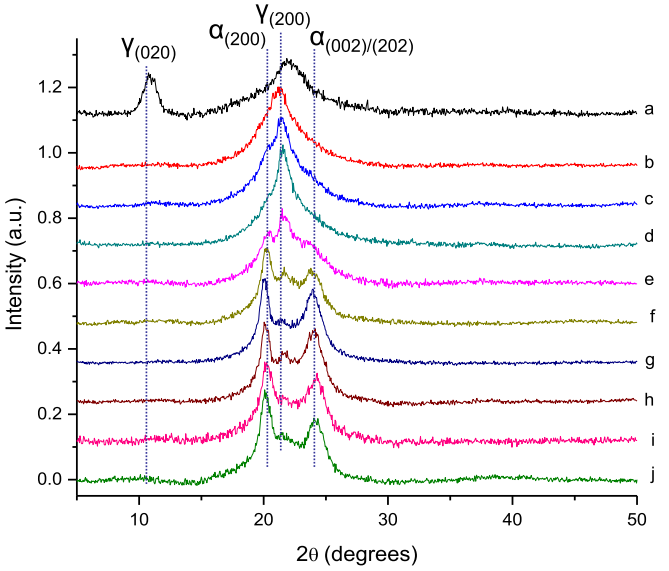

Fig. 6. X-ray profiles of Nylon 6 processed from formic acid: (a) KI/I$_2$ treated cast film; fibers electrospun (b) without the environmental chamber and with varying concentrations of evaporated formic acid: (c) 0 g/m^3, (d) 38 g/m^3, (e) 76 g/m^3, (f) 114 g/m^3, (g) 151 g/m^3, (h) 189 g/m^3, (i) 227 g/m^3; and (j) a solvent cast film.

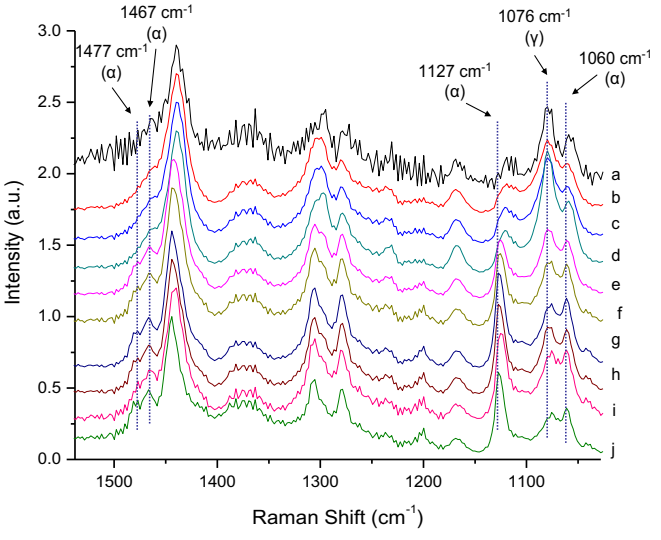

Fig. 7. Raman spectra of Nylon 6 processed from formic acid: (a) KI/I$_2$ treated cast film; fibers electrospun (b) without the environmental chamber and with varying concentrations of evaporated formic acid: (c) 0 g/m^3, (d) 38 g/m^3, (e) 76 g/m^3, (f) 114 g/m^3, (g) 151 g/m^3, (h) 189 g/m^3, (i) 227 g/m^3; and (j) a solvent cast film. All spectra were normalized relative to the 1440 cm^{-1} CH_2 bending vibration.

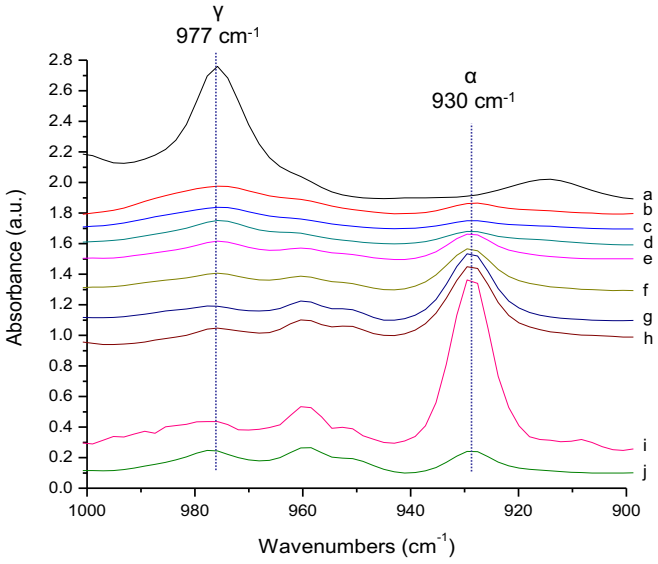

Fig. 8. FTIR spectra of Nylon 6 processed from formic acid: (a) KI/I_2 treated cast film; fibers electrospun (b) without the environmental chamber and with varying concentrations of evaporated formic acid: (c) 0 g/m^3, (d) 38 g/m^3, (e) 76 g/m^3, (f) 114 g/m^3, (g) 151 g/m^3, (h) 189 g/m^3, (i) 227 g/m^3; and (j) a solvent cast film.

also possible that the observed molecular behavior is a result of the solvent vapor transforming the collected fibers as they sit on the collection plate. To investigate this possibility, Nylon 6 was electrospun outside of the environmental chamber and then in separate experiments exposed to HFIP vapor phase concentrations of 121, 137, and 156 g/m^3 for one, two, four, and eight hours to measure the extent of the transformation, if any, of the γ to the α form. The Raman data for the exposure of Nylon 6 to an HFIP concentration of 137 g/m^3 for various times is shown in Fig. 9, where the 1076 cm^{-1} peak is associated with the gauche CC conformation found in the γ form and the 1060 cm^{-1} peak is indicative of the trans amide CC conformation found in the α form.

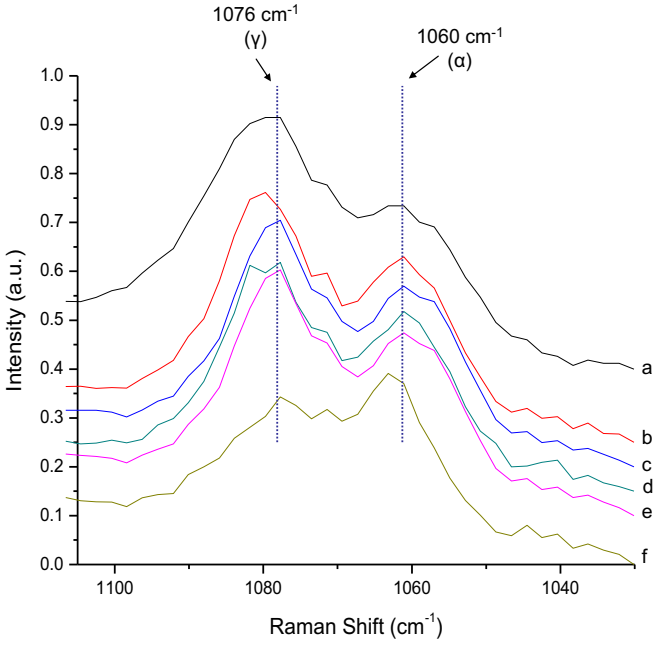

Fig. 9. Raman spectra of Nylon 6 electrospun (a) outside of the chamber and exposed to an HFIP concentration of 137 g/m^3 for (b) 1 h, (c) 2 h, (d) 4 h, (e) 8 h, and (f) electrospun into the chamber with an HFIP concentration of 123 g/m^3.

As can be seen in Fig. 9, the intensity of the 1076 cm^{-1} band is greater than the 1060 cm^{-1} band for the material electrospun outside of the chamber as well as the material exposed to an HFIP concentration of 137 g/m^3 for one, two, four, and eight hours, indicating that the γ form is dominant in these materials. However, the material electrospun inside of the chamber with an HFIP concentration of 123 g/m^3 has a more intense 1060 cm^{-1} band compared to the 1076 cm^{-1} band, suggesting that the α form is dominant. These results suggest that the effect of the solvent vapor on the electrospun material after spinning has a negligible effect on the observed molecular transformation, with a major driving force behind this behavior being the decrease in the solvent evaporation kinetics of electrospinning.

It should be noted that, while this general correlation between the decrease in the rate of evaporation kinetics and the formation of the α form was observed for Nylon 6 electrospun from both HFIP and formic acid, a large degree of variability was observed in the X-ray results obtained at formic acid concentrations of 114, 151, and 189 g/m^3 in the environmental chamber. Three repeats for the case of Nylon 6 electrospun with a formic acid vapor phase concentration of 151 g/m^3, where the material was electrospun on three different days, are shown in Fig. 10. These considerable variations in crystal structure for different trials of Nylon 6 electrospun with the same concentration of formic acid in the environmental chamber can partly be accounted for by the considerable variation in the relative humidity in the laboratory in which the materials were processed. The relative humidity present during the electrospinning experiments with a formic acid concentration of 227 g/m^3 spans a range of about 3%, while the experiments with solvent concentrations of 189, 151, and 114 g/m^3 span a range of 8%, 9%, and 16%, respectively. The trials for lower concentrations of formic acid evaporated within the chamber were not repeated since the (200) reflection of the γ form dominates the diffraction pattern, making any variation in crystal structure difficult to discern.

It is well established that Nylon 6 can absorb water [26–28], with the commonly reported amounts ranging from 1 to 8% (w/w), depending on the relative humidity and pretreatment conditions. It has also been reported that water can affect the γ to α transition observed in Nylon 6 [29]. Thus, it is reasonable to assume that the presence of water can also affect the crystalline state of electrospun

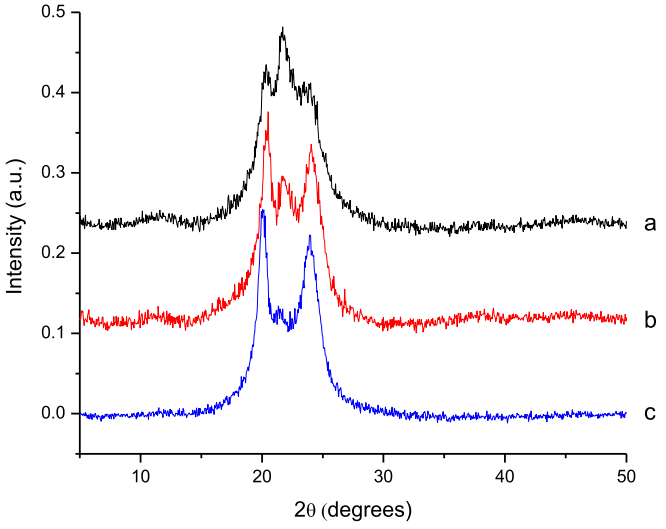

Fig. 10. X-ray profiles of Nylon 6 electrospun with a formic acid concentration of 151 g/m^3 at relative humidities of (a) 26%, (b) 31%, and (c) 17%.

Nylon 6. Given that formic acid and water are miscible due to the efficient formation of hydrogen bonds [30–32], it is likely that the varying amounts of humidity also affected the formic acid evaporation kinetics, which in turn affected the crystalline structure of the electrospun material. Due to the complexity of these interactions, a more rigorous examination is beyond the scope of this study, but is currently being conducted to examine this hypothesis and will be discussed in a future publication.

5. Conclusions

It was shown that, by varying the solvent evaporation kinetics, it is possible to affect the crystal structure of electrospun Nylon 6. A smooth transition between the γ and α crystal forms was observed as the solvent vapor concentration increased. This was observed for Nylon 6 electrospun out of both HFIP and formic acid. For both systems, this transition was most apparent in XRD by observing the increase in intensity of the $(200)_\alpha$ and $(002)_\alpha/(202)_\alpha$ reflections, and the corresponding decrease in intensity of the $(200)_\gamma$ reflection, as increasing amounts of solvent were evaporated in the environmental chamber. Both Raman and FTIR spectroscopy showed analogous changes in the molecular conformation of Nylon 6 associated with the γ and α forms as the solvent concentration increased. More generally, it was shown that, when solvent evaporation occurs on a relatively fast timescale, the γ form appears, whereas slower solvent evaporation results in the α form. A study is currently being conducted to examine whether this behavior is universally observed across all families of polymorphic polymers, and will be discussed in a future publication.

Acknowledgements

The authors acknowledge Dr. Giriprasath Gururajan for help with the electrospinning setup, Mr. Hassnain Jaffari and the Shah lab for use of the XRD system, and Dr. Chao Ni and Mr. Frank Kriss for assistance in acquiring FE-SEM images. In addition, we thank Dr. Steve Givens (E.I. Dupont) for many pertinent discussions. We also acknowledge NSF IGERT 0221651, NSF DMR 0704970, and NSF DMR 0315461 for funding.

References

[1] Holmes DR, Bunn CW, Smith DJ. J Polym Sci Part A Gen Pap 1955;17:159–77.
[2] Arimoto H. J Polym Sci Part A Gen Pap 1964;2:2283–95.
[3] Arimoto H, Ishibash M, Hirai M, Chatani Y. J Polym Sci Part A Gen Pap 1965;3:317–26.
[4] Huang ZM, Zhang YZ, Kotaki M, Ramakrishna S. Compos Sci Technol 2003;63:2223–53.
[5] Greiner A, Wendorff JH. Angew Chem Int Ed 2007;46:5670–703.
[6] Dersch R, Liu TQ, Schaper AK, Greiner A, Wendorff JH. J Polym Sci Part A Polym Chem 2003;41:545–53.
[7] Stephens JS, Chase DB, Rabolt JF. Macromolecules 2004;37:877–81.
[8] Liu Y, Cui L, Guan FX, Gao Y, Hedin NE, Zhu L, Fong H. Macromolecules 2007;40:6283–90.
[9] Li L, Bellan LM, Craighead HG, Frey MW. Polymer 2006;47:6208–17.
[10] Kim GM, Michler GH, Ania F, Calleja FJB. Polymer 2007;48:4814–23.
[11] Stephens JS, Fahnestock SR, Farmer RS, Kiick KL, Chase DB, Rabolt JF. Biomacromolecules 2005;6:1405–13.
[12] Lee KH, Snively CM, Givens S, Chase DB, Rabolt JF. Macromolecules 2007;40:2590–5.
[13] Minato KI, Ohkawa K, Yamamoto H. Macromol Biosci 2006;6:487–95.
[14] Kubono A, Kitoh T, Kajikawa K, Umemoto S, Takezoe H, Fukuda A, Okui N. Jpn J Appl Phys Part 2 1992;31:L1195–7.
[15] McKee MG, Wilkes GL, Colby RH, Long TE. Macromolecules 2004;37:1760–7.
[16] Kawaguchi A. Polymer 1992;33:3981–4.
[17] Murthy NS. J Polym Sci Part B Polym Phys 1986;24:549–61.
[18] Murthy NS. Macromolecules 1987;20:309–16.
[19] Park SY, Cho YH. Macromol Res 2005;13:156–61.
[20] Garreau S, Leclerc M, Errien N, Louarn G. Macromolecules 2003;36:692–7.
[21] Voyiatzis GA, Andrikopoulos KS, Papatheodorou GN, Kamitsos EI, Chryssikos GD, Kapoutsis JA, Anastasiadis SH, Fytas G. Macromolecules 2000;33:5613–23.
[22] Vasanthan N, Salem DR. J Polym Sci Part B Polym Phys 2001;39:536–47.
[23] Rotter G, Ishida H. J Polym Sci Part B Polym Phys 1992;30:489–95.
[24] Reneker DH, Yarin AL, Fong H, Koombhongse S. J Appl Phys 2000;87:4531–47.
[25] Yarin AL, Kataphinan W, Reneker DH. J Appl Phys 2005;98.
[26] Kawasaki K, Kanou K, Sekita Y. J Colloid Sci 1962;17:865–71.
[27] Asada T, Onogi S. J Colloid Sci 1963;18:784–92.
[28] Kawasaki K, Sekita Y. J Polym Sci Part A Gen Pap 1964;2:2437–43.
[29] Miyasaka K, Ishikawa K. J Polym Sci Part A-2 1968;6:1317–29.
[30] Priem D, Ha TK, Bauder A. J Chem Phys 2000;113:169–75.
[31] Aloisio S, Hintze PE, Vaida V. J Phys Chem A 2002;106:363–70.
[32] George L, Sander W. Spectromchim Acta Part A 2004;60:3225–32.